NUMERICAL AND PHYSICAL MODELING OF TURBULENT FLOW AROUND A PLATE WITH TWO TRANSVERSE RIBS

L. G. Artamonova, I. A. Belov,
V. I. Mamchur, A. N. Radtsig,
and L. G. Chernov

UDC 532.517.2

Results are presented of a numerical and experimental investigation of turbulent incompressible fluid flow near a horizontal plate on which one and two interceptors are installed.

The purpose of the investigation is to study the possibility of controlling flow separation on a wall because of the disposition of transverse ribs, interceptors, in the near-wall domain. In contrast to the analysis performed in [1], a difference solution is obtained for the problem posed about the turbulent flow mode, to integrate the system of two-dimensional Reynolds equations in the case of an incompressible fluid which are closed by using a two-parameter dissipative model of turbulence. Besides the numerical modeling of the flow, physical modeling is realized, which consists of building up the flow structure behind the interceptors and measuring the pressure on the surface of the components under consideration in the PT-1 subsonic wind tunnel of the Sergo Ordzhonikidze Moscow Aviation Institute (MAI).

1. Numerical Method of Solution

Under the assumptions made, we write the Reynolds equations in the following generalized form for the variable Φ:

$$\frac{\partial}{\partial x} u\Phi + \frac{\partial}{\partial y} v\Phi - \frac{\partial}{\partial x} \Gamma_\Phi \frac{\partial \Phi}{\partial x} - \frac{\partial}{\partial y} \Gamma_\Phi \frac{\partial \Phi}{\partial y} = S_\Phi. \tag{1}$$

The factor Γ_Φ and the so-called source term S_Φ for the projections of the momentum equation on the x and y axes are written in the form

$$\Phi = u: \Gamma_u = \nu_a + \nu_t = \nu;\ S_u = \frac{\partial}{\partial x}\left(-\frac{p}{\rho} + \nu \frac{\partial u}{\partial x} - \frac{2}{3} k\right) + \frac{\partial}{\partial y} \nu \frac{\partial v}{\partial x};$$

$$\Phi = v: \Gamma_v = \nu;\ S_v = \frac{\partial}{\partial x} \nu \frac{\partial u}{\partial y} + \frac{\partial}{\partial x}\left(-\frac{p}{\rho} + \nu \frac{\partial v}{\partial y} - \frac{2}{3} k\right).$$

Let us note that the continuity equation is obtained from (1) for $\Gamma_\Phi = S_\Phi = 0$.

The equations of the dissipative k–ε-model of turbulence are written with the influence of streamline curvature and physical viscosity in the laminar sublayer, which is substantial for the flow being investigated, taken into account (usually neglected in the standard variation of the k–ε-model, see [2], for example). The streamline curvature is taken into account by representing the term of dissipation generation in the equations for $\tilde{\varepsilon}$ as a function of the turbulent Richardson number $Ri_t = (k/\varepsilon)^2(u_\varepsilon/R_c + \partial u_s/\partial n)(u_s/R_c)$. Such an extension of the dissipative model of turbulence to the case of curved flows is similar to that proposed in [3] (in this paper the dependence of the dissipation term in the equations for ε on Ri_t is introduced), but it permits a more logical construction of the difference solution procedure for the equation for ε that results in a substantial (up to 50%) reduction in computations times on an electronic computer, as is shown by practice. As regards taking account of the influence of the physical viscosity on the turbulent transfer process, then in this analysis the extension of the standard variation of the dissipative model of turbulence to the case of the flow under consideration is realized analogously to what was done in [4].

Sergo Ordzhonikidze Moscow Aviation Institute. Translated from Inzhenerno-Fizicheskii Zhurnal, Vol. 52, No. 1, pp. 43-51, January, 1987. Original article submitted November 15, 1985.

0022-0841/87/5201-0033$12.50

Finally, the factor Γ_Φ and the source terms S_Φ for the turbulence characteristics k and ε, as well as the relationship closing the turbulence model for ν_t have the form

$$\Phi = k\colon \Gamma_k = \nu_a + \frac{\nu_t}{\sigma_k};\ S_k = P_k - \rho\varepsilon;\ \Phi = \varepsilon\colon \Gamma_\varepsilon = \nu_a + \frac{\nu_t}{\sigma_\varepsilon};$$
$$S_\varepsilon = c_1(1 + c_w \mathrm{Ri}_t)\frac{\hat{\varepsilon}}{k}P_k - c_2 f_2 \frac{\hat{\varepsilon}^2}{k};\quad \nu_t = c_\mu f_\mu \frac{k^2}{\varepsilon}, \tag{2}$$

where $c_1 = 1.45$; $c_2 = 1.92$; $c_\mu = 0.09$; $\sigma_k = 1$; $\sigma_\varepsilon = 1.3$; $c_w = 0.2$ are constants of the turbulence model, $P_k = \nu_t\{2[(\partial u/\partial x)^2 + (\partial v/\partial y)^2] + (\partial u/\partial y + \partial v/\partial x)^2\}$; $f_2 = 1 - 0.3\exp(-\mathrm{Re}^2_t)$; $f_\mu = \exp[-2.5/(1 + \mathrm{Re}_t/50)]$; $\mathrm{Re}_t = k^2/(\nu_a\varepsilon)$; $\hat{\varepsilon} = \varepsilon - 2\nu_a(\partial k^{1/2}/\partial n_w)^2$; and n_w is the normal to the wall.

The formulation of the conditions on all the boundaries of the computational domain, with the exception of the solid surface, is evident (see [5], for example). Values of the desired parameters near the wall are found from the solutions of the corresponding original equations, taking into account the experimentally verified assumptions that if the ordinate of the near-wall node is $y_1 < \delta/4$, then in the equations for the longitudinal velocity component the diffusion and the work of the pressure forces are governing in the section $y = [0, y_1]$, the generation and dissipation terms predominate in the equation for k in the same section in the domain of developed turbulence, while in addition the diffusion terms also predominate in the equation for ε. The following distributions $k \sim y^2$; $\varepsilon \sim y$; $\nu_t \sim y^3$ are valid in the viscous sublayer domain. In comparison with the method of near-wall functions usually utilized in numerical computations (see [6], for example), the approach described permits computation of the flow section near the wall more accurately and with physical foundation for the flows under investigation that are characterized by the substantial influence of physical viscosity and longitudinal pressure gradients in individual domains and, moreover, does not require a large quantity of difference mesh nodes on this section, which results in a significent saving in the computation time as a whole.

Methodological computations performed have shown that utilization of a "hybrid" difference scheme [5] combining central differences of second order accuracy and first order counterflow differences to solve the initial system of equations and schemes [6] of elevated order of accuracy yields sufficiently close results for the flow under consideration. Consequently, mainly the more economical "hybrid" scheme was later used in the computations.

2. Flow around a Plate with One Interceptor

All the computations presented below were performed for $\mathrm{Re}_h = u_\infty h/\nu_a = 10^5$, $\delta_i/h = 0.4$. The distance between the upstream edge of the plate and the site of interceptor disposition $L_{in} = 15h$ corresponds to the quantity δ_i/h taken. Downstream the plate is assumed unlimited while the distance between the interceptor and the outlet boundary of the computational domain is selected ($L_{out} = 25h$) so as to assure weak influence of the outlet boundary on the flow near the interceptor. In order to compare the computed and experimental data, the turbulence characteristics in the free stream were determined by means of the corresponding parameters of the experimental installation: the turbulence scale ℓ was assumed equal to the size of the honeycomb cell (50 × 50 mm), the mean intensity of the turbulence defined as $(\sqrt{k}/u)_\infty$ was considered given ($\sqrt{k_\infty} = 0.001u_\infty$). Then, in conformity with the Kolmogorov–Prandtl formula, the coefficient of turbulent viscosity in the unperturbed flow equals the product $\sqrt{k_\infty}\ell$, from which we have $\varepsilon_\infty = c_\infty k_\infty^{3/2}/\ell$ if the relationship for $\nu_{t\infty}$ prescribed by the dissipative model of turbulence is taken into account. For $\mathrm{Re}_h = 10^5$ and $u_\infty = 50$ m/sec for air ($\nu_a = 1.5\cdot10^{-5}$ m^2/sec) in this case $k_\infty = 10^{-6}u^2_\infty$; $\varepsilon_\infty = 0.054\cdot10^{-9}(u^3_\infty/h)$; $\nu_{t\infty} = 0.00167u_\infty h$.

It follows from Fig. 1a that the flow around the interceptor is, as also in the laminar model (see [1]), accompanied by the formation of a complex vortex structure in which three kinds of reverse flows are isolated: the leading vortex 1, the large-scale main vortex 2 elongated in the longitudinal direction and the secondary vortex 3 within it. To estimate the intensities of the mentioned separation flows, the value of the minimal flow rate is selected in the appropriate flow $\Psi_m = \int_0^y u dy/(u_\infty h)$. To a definite degree the intensity can be estimated by the maximum velocity u_m of the reverse flow in the vortex. The most intensive of the vortices being formed during the flow around the interceptor is the main vortex (Ψ_m =

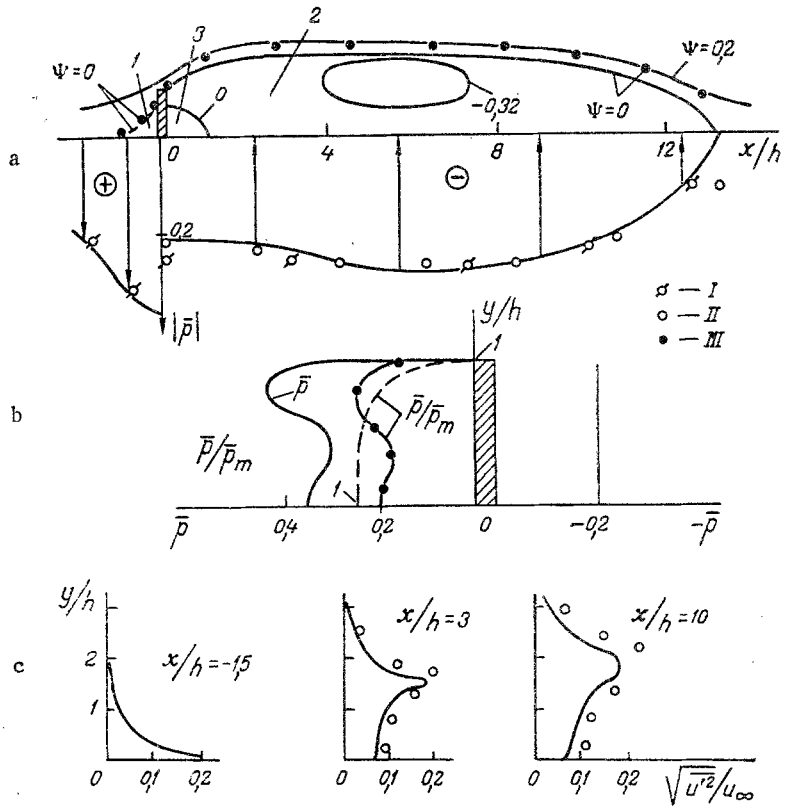

Fig. 1. Flow around a plate with one interceptor ($Re_h = 10^5$): solid curve is the computation; experiment: I) authors' data; II) [7], III) [9]; dashed curve is for an isolated interceptor (data of [8]).

-0.38; $u_m = 0.58u_\infty$). The leading vortex is characterized by a lower intensity ($\Psi_{m\ell} = -0.07$; $u_{m\ell} = 0.3u_\infty$). The intensity of the secondary vortex is not great.

The large boundary layer thickness, as well as the presence of the leading vortex, result in a substantial qualitative and quantitative redistribution of the pressure along the forward endface of the interceptor as compared with the case of the flow around it in the absence of a horizontal plate, see Fig. 1b, where $\bar{p} = (p - p_\infty)/(\rho u^2_\infty)$, although the integral magnitude of the drag coefficient of the interceptor leading endface $C_{x\ell}$ varies insignificantly with respect to the case mentioned and equals ≈ 0.73 (this, as well as the remaining drag coefficients, is normalized with respect to the velocity u_∞ and the dimension h). To a somewhat greater extent, the presence of the plate is perceived by the magnitude of the pressure in the flow near the trailing edge of the interceptor, which results, in particular, in a reduction in the corresponding (bottom) drag coefficient C_{xd} by almost 25%: $C_{xd} = 0.42$. As computations show, for the chosen values of the geometric parameters L_{in}/h and L_{out}/h the negative friction, in sign, on the reverse flow sections is equilibrated approximately by the positive friction in the remaining near-wall domains of the plate, in which connection, we later neglect the contribution of plate friction to the total drag of the plate-interceptor components (this is also valid in the case considered below of the flow over a plate with two interceptors). Taking the above into account, the drag coefficient of the component being investigated is $C_x = 1.15$. The developed nature of the circulation flow in the wake behind the interceptor results in strong rarefaction of the flow in this domain, whereupon lift (a transverse load) occurs on the plate under the condition that $p = p_\infty$ on the lower surface of the plate. Let us note that lift occurs when the main fluid motion is in the direction along the plate, i.e., when the plate is at a zero angle of attack with respect to the free stream. The lift coefficient of the plate-interceptor configuration is here $C_y = 2.2$ and its aerodynamic quality is $K = C_y/C_x = 1.9$.

As follows from Fig. 1c, the flow in the wake behind the interceptor is accompanied on its main part by a high level of turbulent fluctuations, whose maximal quantities are observed in the mixing layer of the main vortex. According to computations, the flow is close to laminar only in the area of the secondary vortex. In the space ahead of the inter-

ceptor the domain of intense flow turbulence is localized by the leading vortex, and upstream by a comparatively thin section of the plate boundary layer.

Attention is turned in Fig. 1 to the satisfactory agreement between the results of a computation and the data of experiment, including in such "fine" flow characteristics as the distribution of turbulent correlations and the configuration of individual separation flow domains. Let us also note the sufficiently good correspondence between the experimental surface pressure distributions in the wake behind the interceptor obtained in the present investigation and in [7].

3. Flow around a Plate with Two Interceptors

We make the configuration examined earlier more complicated by arranging another interceptor of height h_1 (we call it first) upstream of the interceptor of height h (we call it the second interceptor) at a distance of L = 4h away. Computations show that if the influence of the first interceptor on the flow pattern of the second is not large for $h_1/h \leqslant 0.25$, then for a value of $h_1/h = 0.4$, a noticeable rearrangement of the flow is already observed around the interceptor system, which is caused by the formation of a developed circulation flow in the space between them for which $\Psi_{m_1} = -0.13$; $u_{m_1} = 0.3u_\infty$ (Fig. 2a). A result is a sharp reduction in the pressure ahead of the second interceptor as compared with the case of isolated flow, and a smoother flow of the stream around this interceptor, which results in particular to attenuation of the intensity ($\Psi_{m_2} = -0.15$; $u_{m_2} = 0.45u_\infty$) and diminution in the size of the main vortex as well as in the pressure behind this interceptor. Because of such flow transformations, the drag coefficients are reduced significantly for the leading (becomes negative) and trailing endfaces of the second interceptor $C_{x\ell_2} = -0.05$; $C_{xd_2} = 0.33$. Therefore, the total drag of the interceptor mentioned is diminished by more than four times as compared with the case of its isolated flow: $C_{x_2} = 0.28$. Since the drag of the first interceptor is not large in connection with the relative smallness of its size: $C_{x_1} = 0.33$, the drag of the configuration under consideration $C_x = C_{x_1} + C_{x_2} = 0.61$ turns out to be 1.9 times lower than the drag of the configuration with one interceptor. Let us note that an analogous effect was obtained in [8] in an analysis of the flow around a set of two plates of different size.

Because of the stronger drop in rarefaction in the near wake behind the second interceptor as compared with the diminution in the positive pressure ahead of it, the lift of a configuration consisting of two interceptors on a plate is lower than for the configuration with one interceptor: $C_y = 1.3$; its aerodynamic quality is nevertheless elevated (K = 2.15).

The attenuation remarked above in the stall of the stream from the sharp edge of the second interceptor is the reason for the diminution in the intensity of the turbulent fluctuations in the wake behind this interceptor (the fluctuation level in this domain does not exceed the turbulent fluctuation level in the space between the interceptors (see Fig. 2b)).

As the parameter h_1/h grows to 0.6 the intensity of the vortex between the interceptors ($\Psi_{m_1} = -0.17$; $u_{m_1} = 0.33u_\infty$) as well as its size increase, resulting in a further development of the hydrodynamic processes described above (see Fig. 2c). In particular, rarefaction of the stream in the space between the interceptors grows while it diminished behind the second. As a result, the drag of the second interceptor is reduced almost to zero, and although the drag of the first interceptor grows to $C_{x_1} = 0.52$ because of the growth in its size and the increase in the base drag C_{xd_1}, the total drag of the configuration continues to drop (C_x = 0.53). Despite the substantial redistribution of the pressure over the plate surface as compared with the case $h_1/h = 0.4$, the coefficient C_y of the configuration remains practically invariant, which is associated with the approximately identical growth of the rarefaction of the stream in the space between the interceptors with respect to the increase in surface pressure on the remaining part of the plate. As h_1/h changes from 0.4 to 0.6 the quality of the configuration grows negligibly (around 10%).

As the parameter h_1/h grows to 0.7 (Fig. 2d) the intensity of the vortex enclosed between the interceptors becomes so high ($\Psi_{m_1} = -0.145$; $u_{m_1} = 0.4u_\infty$) that the level of stream rarefaction in the corresponding domain turns out to be higher than in the near wake behind an isolated streamlined interceptor (for instance, the coefficient $C_{xd_1} = 0.46$ in the case under consideration). This, as well as the rise in the drag of the leading endface of the first interceptor, results in the increase in the coefficient C_{x_1} starting to lead the diminution in the coefficient C_{x_2} ($C_{x_1} = 0.73$, $C_{x_2} = -0.17$) and the total drag of the configuration grows: $C_x = 0.56$. Let us note the occurrence of a force, directed upsteam, on the second

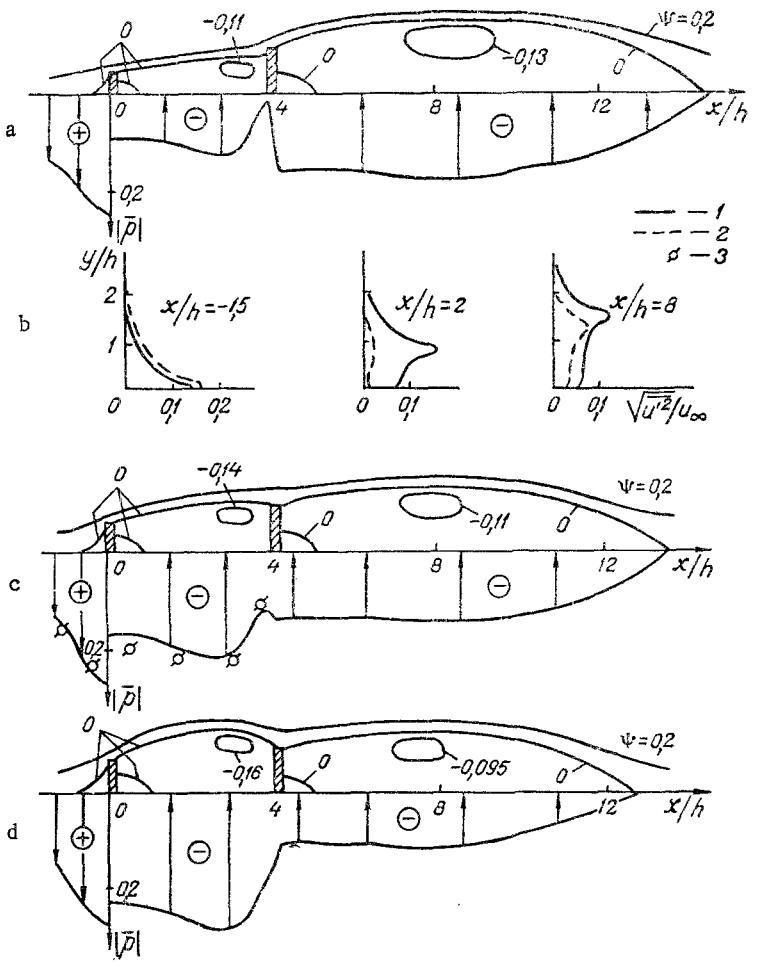

Fig. 2. Flow around a plate with two interceptors ($Re_h = 10^5$; $L/h = 4$): 1 and 2) computation; a) $h_1/h = 0.4$; b) $h_1/h = 0.4$ (1) and 0.7 (2); c) $h_1/h = 0.6$; 3) experiment (authors' data); d) $h_1/h = 0.7$.

interceptor for $h_1/h = 0.7$. As before, the left and quality of the configuration vary insignificantly ($C_y = 1.3$, $K = 2.3$).

It follows from computations that the growth of the parameter h_1/h is accompanied by attenuation of the turbulent fluctuation level in the whole flow domain downstream behind the first interceptor (see Fig. 2b). This process is especially definite in the gap between the interceptors where the turbulence intensity is reduced by more than an order of magnitude as h_1/h changes from 0.4 to 0.7 (for $h_1/h = 0.7$ the values of the turbulence parameters in the domain mentioned are close to the corresponding values in the free stream). The reason for this is the increase in curviness of the streamlines in the domain between the interceptors as h_1/h grows (see the dependence (2) while taking into account that $Ri_t > 0$ here). A diminution in the turbulent fluctuation level in the wake behind the second interceptor as h_1/h grows is explained by the attenuation of the stream stall on this interceptor here. The intensity of the turbulence upstream of the first interceptor changes to a much lesser degree depending on the parameter h_1/h (see Fig. 2b).

As h_1/h increases approximately to the value 0.85 the flow near the system of two interceptors on a plate is reconstructed qualitatively for a given distance L/h and the second interceptor turns out to be entirely in the domain of the main vortex being developed behind the first interceptor. This regime of flow around the configuration is accompanied by a further rise in its drag as h_1/h increases (the increase in the coefficient C_x anticipates the drop in the coefficient C_{x_2}). The lift of the configuration increases in this case because of the magnification of the stream rarefaction behind the first interceptor, and its aerodynamic quality here changes negligibly.

As is seen from Fig. 3a, for the selected value of $L/h = 4$ the optimal configuration from the viewpoint of obtaining minimum drag, that consists of two interceptors arranged on a plate, holds for $h_1/h = 0.6$. The drag of such a configuration, equal to 0.53, is more

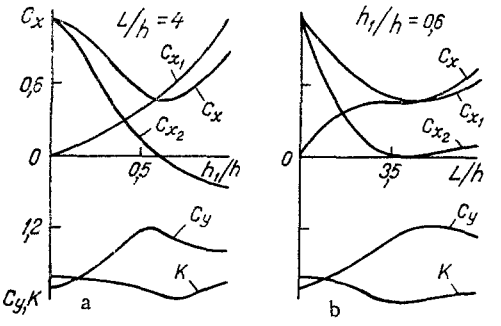

Fig. 3

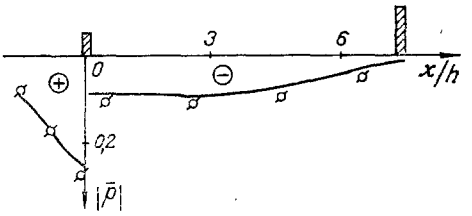

Fig. 4

Fig. 3. Dependence of the aerodynamic coefficients of the plate-interceptor configuration on the geometric dimensions of the configuration for $Re_h = 10^5$.

Fig. 4. Comparison of the results of theory and experiment for the flow around a plate with two interceptors for $Re_h = 10^5$, $h_1/h = 0.4$, $L/h = 7.5$. The curves are theory, the points are experiment (authors' data).

than two times less, while the quality, equal to 2.35, is almost 25% greater than the corresponding indices for a configuration with one interceptor. The configuration of optimal quality ($K = 2.4$ for $h_1/h = 0.7$) also has a similar geometry. Let us note that for $L/h = 4$ in a laminar flow mode ($Re_h = 10^3$) $h_1/h = 0.75$; here $C_x = 0.35$ and $K = 3.0$ [1].

As the parameter h_1/h changes the qualitative regularities of the flow under investigation remain entirely as before for different fixed values of the relative distance between the interceptors in the range $L/h \leq 7$. In the case $3 \leqq L/h \leqq 7$, the influence of the parameter L/h on the nature of the flow around the configuration is not large depending on h_1/h (Fig. 3b), the hydrodynamic processes described above proceed more slowly with the growth of h_1/h for other values of L/h from the range mentioned than for $L/h = 4$. Let us note the weak dependence of the quality of the configuration on the parameter L/h that follows from Fig. 3b.

It follows from an analysis of the computed results in the whole considered range of variation of the geometric parameters h_1/h and L/h that for the values of Re_h and δ_i/h given in the computation the plate with two interceptors installed is a logical configuration for drag when approximately $h_1/h = 0.6$-0.65 and $L/h = 3.5$-5 and for aerodynamic quality when $h_1/h = 0.6$-0.8 and $L/h = 2.5$-7. Therefore, a configuration optimal in both parameters has the following dimensions: $h_1/h = 0.6$-0.65 and $L/h = 3.5$-5. The drag of such a configuration is not less than two times lower while the quality is not less than 20% better as compared with the plate-interceptor configuration.

A confirmation of the confidence of the obtained computational results is their satisfactory agreement with the data of experiment performed both for configurations close to the optimal (see Fig. 2c) and for those that differ (Fig. 4). It is interesting to note the weak influence (according to the computations) of the Reynolds number on the aerodynamic characteristics of the considered configurations for $Re_h > 10^5$, which is apparently related to the developed nature of the turbulent processes proceeding in the reverse flow domain near the plate surface, which is due, in turn, to the sufficiently intense stall of the stream on the interceptors.

NOTATION

x, y, coordinates (along and normal to the plate); n, normal direction to the streamline; R_c, streamline radius of curvature; h, interceptor height (the second interceptor in the stream); h_1, height of the first interceptor in the stream; L, spacing between interceptors; δ, boundary layer thickness on the plate; δ_i, boundary layer thickness on a plate in the absence of an interceptor; y_1, ordinate of the first near-wall node of the difference mesh; L_{in}, distance between the interceptor (first interceptor) and the input boundary of the computational domain; L_{out}, distance between the interceptor (second interceptor) and the output boundary of the computational domain; u, v, velocity components in the x and y directions, respectively; u_s, fluid velocity along a streamline; u_m, maximal reverse flow velocity; p, pressure; p_m, maximal pressure on the leading endface of the interceptor; ρ, density; $\bar{p}$, dimensionless pressure, $\bar{p} = (p - p_\infty)/(\rho u^2_\infty)$; k, kinetic energy of the turbulent fluctuations;

ε, rate of dissipation of this energy; ν_a, ν_t, ν, kinematic, turbulent, and effective viscosities, respectively; Ψ, stream function; Ψ_m, minimum flow rate in the appropriate flow; C_{x_ℓ}, C_{x_d}, drag coefficients of the leading and trailing endfaces of the interceptor (normalized with respect to the velocity head of the unperturbed stream and the interceptor height h); C_{x_1}, C_{x_2}, drag coefficients of the first and second interceptors; C_x, total drag coefficient of the configuration; C_y, configuration lift coefficient; K, configuration aerodynamic quality; Re_h, Reynolds number; Ri_t, Richardson number; Re_t, turbulent Reynolds number; c_1, c_2, c_μ, σ_k, σ_ε, c_w, f_2, f_μ, constants and empirical functions governing the turbulence model. Subscripts: ∞, unperturbed flow; 1, the vortex ahead of the interceptor on the free stream side; 2, the main vortex in the wake behind the interceptor.

LITERATURE CITED

1. I. A. Belov and V. I. Mamchur, Uch. Zap. TsAGI, 16, No. 2, 93-97 (1985).
2. W. Colman (ed.), Turbulent Flow Computation Methods [Russian translation], Moscow (1984).
3. Londer, Pridden, Sharma, Theoretical Principles of Engineering Computations [Russian translation], No. 1, 332-342 (1977).
4. J. A. Humphrey, J. Whitelaw, and G. Yee, J. Fluid Mech., 103, 443-463 (1981).
5. N. A. Kudryavtsev, Numerical Analysis of the Flow around a Disc by a Turbulent Incompressible Fluid Flow [in Russian], Deposited paper No. 4465-82 Dep., VINITI, Moscow (1982).
6. N. Leschtsiner and W. Roddy, Theoretical Principles of Engineering Computations [Russian translation], 103, No. 2, 299-307 (1981).
7. E. V. Vlasov, A. S. Ginevskii, R. K. Karavosov, and M. O. Frankfurt, Trudy TsAGI, No. 2137, 3-32 (1982).
8. I. A. Belov, Zh. Prikl. Mekh. Tekh. Fiz., No. 4, 107-109 (1980).
9. M. C. Good and P. N. Joubert, J. Fluid Mech., 31, 547-570 (1968).

THE EFFECT OF THERMAL SELF-ACTION OF A LIGHT BEAM IN A SHEAR FLOW

M. N. Kogan, A. N. Kucherov, and M. V. Ustinov

UDC 535.211+533.6

The effect of thermal self-action in a shear gas flow transverse to the beam and containing a stagnation domain is investigated.

The effect of thermal blooming of a radiation beam in a moving self-absorbing medium was examined earlier for the case of a homogeneous uniform flow [1, 2]. A classification is introduced for the light beam blooming modes in the gas flow as a function of the magnitude of the stream velocity component transverse to the beam [3]. In a medium at rest and in a slow stream (the heat conducting mode and the forced convection mode) a beam with an initially Gaussian distribution is defocused, as a rule, if the index of refraction of the medium diminishes as the temperature rises (water, air and other media). At high stream velocities when pressure perturbations become substantial, focusing the beam in a gaseous medium becomes possible because of the thermal blooming.

The effect exerts extreme action on the beam in an unsteady flow (at the initial time interval after switching in the beam). For instance, the peak intensity reaches a maximum or minimum depending on just how the gasdynamic blooming mode is considered [4, 5].

The effect of thermal blooming is investigated in this paper in a shear flow when the velocity changes its magnitude in distances on the order of the beam dimension.

We direct the z coordinate along the beam, the x coordinate in the stream direction. We assume the magnitude of the stream velocity to depend only on the transverse coordinate y ($\mathbf{V} = \mathbf{i}\, U_0 U(y)$, where $\mathbf{V}$ is the velocity vector, $\mathbf{i}$ is the unit direction along the x axis, $U(y)$ is a given function, and U_0 is the characteristic magnitude of the velocity), while

Translated from Inzhenerno-Fizicheskii Zhurnal, Vol. 52, No. 1, pp. 51-56, January, 1987. Original article submitted August 29, 1985.